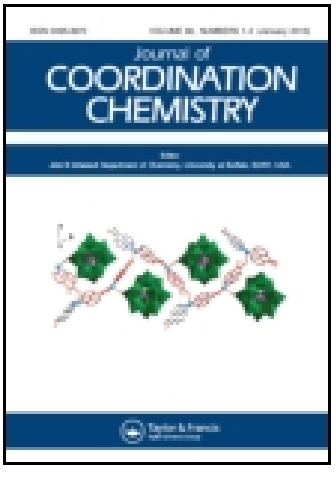

Journal of Coordination Chemistry
Publication details, including instructions for authors and subscription information:
http://www.tandfonline.com/loi/gcoo20

Binuclear ruthenium complexes containing mPTA and alkyl-bis(8-thiotheophylline) derivatives (mPTA = N-methyl-1,3,5-triaza-7-phosphaadamantane)

Lazhar Hajji[a], Cristobal Saraiba-Bello[a], Manuel Serrano-Ruiz[a] & Antonio Romerosa[a]

[a] Facultad de Ciencias Experimentales, Área de Química Inorgánica-CIESOL, Universidad de Almería, Almería, Spain

Accepted author version posted online: 25 Jul 2014.Published online: 11 Sep 2014.

To cite this article: Lazhar Hajji, Cristobal Saraiba-Bello, Manuel Serrano-Ruiz & Antonio Romerosa (2014) Binuclear ruthenium complexes containing mPTA and alkyl-bis(8-thiotheophylline) derivatives (mPTA = N-methyl-1,3,5-triaza-7-phosphaadamantane), Journal of Coordination Chemistry, 67:16, 2701-2710, DOI: 10.1080/00958972.2014.947970

To link to this article: http://dx.doi.org/10.1080/00958972.2014.947970

Journal of Coordination Chemistry, 2014
Vol. 67, No. 16, 2701–2710, http://dx.doi.org/10.1080/00958972.2014.947970

Binuclear ruthenium complexes containing mPTA and alkyl-bis(8-thiotheophylline) derivatives (mPTA = N-methyl-1,3,5-triaza-7-phosphaadamantane)

LAZHAR HAJJI, CRISTOBAL SARAIBA-BELLO, MANUEL SERRANO-RUIZ and ANTONIO ROMEROSA*

Facultad de Ciencias Experimentales, Área de Química Inorgánica-CIESOL, Universidad de Almería, Almería, Spain

(*Received 15 May 2014; accepted 8 July 2014*)

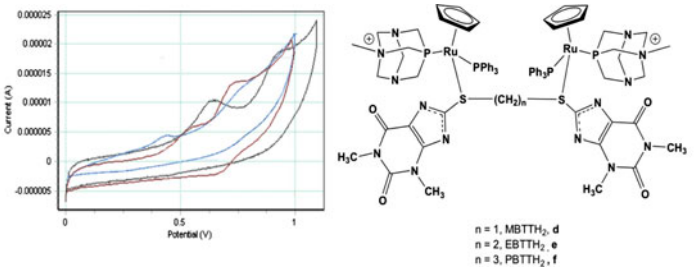

The water-soluble complex $[RuClCp(PPh_3)(mPTA)](CF_3SO_3)$ reacts with the thiopurines, bis(S-8-thiotheophylline)methane ($MBTTH_2$), 1,2-bis(S-8-thiotheophylline)ethane ($EBTTH_2$), and 1,3-bis(S-8-thiotheophylline)propane ($PBTTH_2$), to lead to the binuclear ruthenium(II) complexes $[\{RuCp(PPh_3)(mPTA)\}_2\text{-}\mu\text{-}(L\text{-}\kappa S7,S'7)](CF_3SO_3)_2$ where (L = $MBTT^{2-}$ (**1**), $EBTT^{2-}$ (**2**), and $PBTT^{2-}$ (**3**)). All the complexes have been fully characterized by elemental analysis, IR, and multinuclear ^1H, $^{13}C\{^1H\}$, and $^{31}P\{^1H\}$ NMR spectroscopy. The cyclic voltammetry of the complexes is characterized by two one-electron oxidative responses (Ru^{II}–Ru^{II}/Ru^{III}–Ru^{II}; Ru^{III}–Ru^{II}/Ru^{III}–Ru^{III}) that increase their redox potential when the bis(8-thiotheophylline)-alkyl-bridge growths. The reactivity against DNA and partition coefficient of the complexes were also determined.

Keywords: Ruthenium complexes; Bisthiotheophylline; Metal–purine interaction; Metal–phosphine complexes; Water-soluble complexes; Electrochemistry

1. Introduction

After the discovery of the anticancer properties of *cis*platin in the 1960s by Rosenberg [1], metal compounds of wide structural diversity have been tested as therapeutic agents for cancer treatment [2–10]. Nevertheless, the utility of platinum complexes [11], they have important disadvantages like toxicity and drug resistance [12, 13]. An interesting alternative

*Corresponding author. Email: romerosa@ual.es

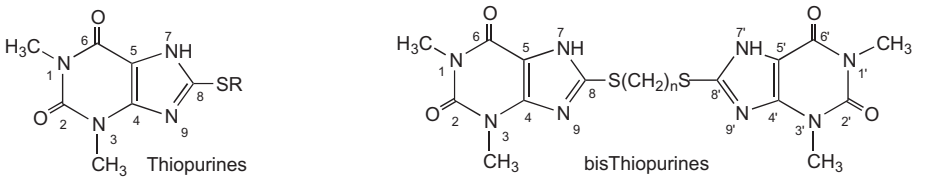

R = H, 8-TTH$_2$ **a**
R = Me, 8- MTTH, **b**
R = CH_2Ph, 8- BzTTH, **c**

n = 1, MBTTH$_2$, **d**
n = 2, EBTTH$_2$, **e**
n = 3, PBTTH$_2$, **f**

Scheme 1. Chemical structure of thiopurines and bisthiopurines.

is ruthenium complexes [14–19] as two of them, NAMI-A [20, 21] and KP1019 [22] are water-soluble and are currently under clinical trials.

We have obtained water-soluble platinum [23, 24] and ruthenium [25] complexes containing the water-soluble phosphine PTA and its derivatives mPTA and dmPTA (PTA = 1,3,5-triaza-7-phosphaadamantane; mPTA = *N*-methyl-1,3,5-triaza-7-phosphaadamantane; dmPTA = *N,N′*-dimethyl-1,3,5-triaza-7-phosphaadamantane) [26–29], some with significant anticancer activity on live cells. In order to obtain information on how these ruthenium complexes interact with purines, they were reacted with thio- and in particular, with bisthio-purines (scheme 1). The bisthio-purines are particularly interesting compounds as they bear two coordination sites at a variable distance depending on the length of the spacing group. In fact, the coordination of the metal to a ligand site could favor coordination of the second nucleus on the other one, or on the contrary, the two sites could display an independent reactivity, similar to that in nucleotides. Cooperative or synergic effects of the two metal nuclei could amplify the antiproliferative activity.

In a previous paper, we showed that the water-soluble ruthenium(II) mononuclear complexes [RuClCp(PTA)(L)] provided mononuclear [RuCp(X-κ*S*)(PTA)(L)] and binuclear complexes [{RuCp(PTA)(L)}$_2$-μ-(Y-κ*S,S′*)] (X = 8-thio-theophyllinates from **a** to **c**; Y = 8-thio-theophyllinates from **d** to **f**; L = PTA, L = PPh_3). The observed antiproliferative activities of the complexes on *cis*platin-sensitive T2 and *cis*platin-resistant SKOV3 cell lines were correlated with their 1-octanol–water partition coefficient [30]. The data supported the hypothesis that the liphophilic/hydrophilic balance could be a determining factor inside these Ru complexes.

A new combination of phosphines with different water/organic solvent solubility properties should be checked to determine if the partition coefficient is the main factor that justifies the observed poor activity of the bispurine–ruthenium complexes containing PTA and PPh_3.

In this paper, we present the synthesis and characterization of three new products obtained by reaction of the cationic starting complex $[RuClCp(PPh_3)(mPTA)]^+$ with the bisthiopurines $MBTT^{2-}$ (**d**), $EBTT^{2-}$ (**e**), and $PBTT^{2-}$ (**f**), and the study of their reactivity with DNA, partition coefficient, and redox properties.

2. Experimental

2.1. *General procedures*

All reactions and manipulations were routinely performed under a dry nitrogen atmosphere using standard Schlenk-tube techniques. All chemicals were of reagent grade and used as

received by commercial suppliers unless otherwise stated. The solvents were all degassed and distilled according to standard procedures [31]. The compounds mPTA, [RuClCp(PPh_3)(mPTA)](CF_3SO_3) and bis(8-thiotheophylline) alkane derivatives MBTTH, EBTTH, and PBTTH were prepared following the procedure described [32–37]. Solvents for NMR measurements (Cortec-Euriso-top) were dried over molecular sieves (0.4 nm). ^{1}H, ^{31}P{^{1}H} NMR, and ^{13}C{^{1}H} NMR spectra were recorded on a Bruker DRX300 spectrometer operating at 300.13 MHz (^{1}H), 121.49 MHz (^{31}P), and 75.47 MHz (^{13}C), respectively. Peak positions are relative to tetramethylsilane and were calibrated against the residual solvent resonance (^{1}H) or the deuterated solvent multiplet (^{13}C). Chemical shifts for ^{31}P{^{1}H} NMR spectra were measured relative to external 85% H_3PO_4 with downfield values taken as positive. Infrared spectra were recorded on KBr disks using an FT-IR ATI Mattson Infinity Series. Elemental analysis (C, H, N, S) was performed on a Fisons Instruments EA1108 elemental analyzer.

2.2. *Synthesis of [{RuCp(PPh$_3$)(mPTA)}$_2$-μ-(MBTT-κS7,S′7)](CF$_3$SO$_3$)$_2$ (1)*

$MBTTH_2$ (0.015 g, 0.0344 mM) was dissolved in 10 mL of KOH ethanolic solution (0.0075 M) and reacted with [RuClCp(PPh_3)(mPTA)](CF_3SO_3) (0.054 g, 0.0688 mM). After refluxing for 4 h, the resulting solution was filtered at room temperature and concentrated under reduced pressure to 1 mL. The yellow precipitate was filtered, washed with Et_2O (2 × 2 mL), and finally dried under vacuum.

Yield: 54 mg, 82%. $S_{25,H2O}$ (mg/cm^3): 0.8. Log *P*: 0.94. Elemental analysis for $C_{77}H_{84}F_6N_{14}O_{10}P_4Ru_2S_4$ (1933.87 g M^{-1}): Found C, 47.85; H, 4.48; N, 10.03; S, 6.53%; Calcd C, 47.82; H, 4.37; N, 10.14; S, 6.63%.

IR (KBr, cm^{-1}): *ν*(C6=O) 1681 (s); *ν*(C2=O) 1637 (s); *ν*(C=C+C=N) 1521 (s); *ν*(SO) 1226 (s); ^{1}H NMR (20 °C, DMSO-d$_6$): *δ* 2.74 (s, C**H**$_3$N$_{mPTA}$, 6H); 3.20 (s, N1–C**H**$_{3(MBTT)}$, 6H); 3.35 (s, N3–C**H**$_{3(MBTT)}$, 6H); 3.39–4.24 (m, C**H**$_2$P$_{mPTA}$, 12H); 4.68 (bs, S–C**H**$_{2(MBTT)}$, 2H); 4.88–5.02 (m, C**H**$_2$N$_{mPTA}$, 12H); 5.27 (s, Cp, 10H); 7.20–7.58 (m, aromatics, 30H). ^{13}C{^{1}H} NMR (20 °C, DMSO-d$_6$): *δ* 27.87 (s, N1–CH$_{3(MBTT)}$); 30.28 (s, N3–**C**H$_{3(MBTT)}$); 35.53 (s, S–**C**H$_{2(MBTT)}$); 48.98 (s, **C**H$_3$N$_{mPTA}$); 50.21 (d, $^1J_{CP}$ = 12.52 Hz, N**C**H$_2$P$_{mPTA}$); 51.27 (d, $^1J_{CP}$ = 15.87 Hz, CH$_3$N**C**H$_2$P$_{mPTA}$); 59.78 (s, N**C**H$_2$N$_{mPTA}$); 68.55 (s, CH$_3$N**C**H$_2$N$_{mPTA}$); 85.80 (s, C$_p$); 119.55 (q, $^1J_{CF}$ = 316.52 Hz, OSO_2CF_3); 115.44 (s, C5); 129.40–133.86 (m, aromatics); 150.88 (s, C4); 151.12 (s, C8); 151.78 (s, C6); 156.34 (s, C2). ^{31}P{^{1}H} NMR (20 °C, DMSO-d$_6$): *δ* 42.60 (d, $^2J_{PP}$ = 38.52 Hz); −17.95 (d, $^2J_{PP}$ = 38.52 Hz). Cyclic voltammetry (DMF, 22 °C): $E_{ox(1)}$ = 0.635 mV; $E_{ox(2)}$ = 0.920 mV.

2.3. *Synthesis of [{RuCp(PPh$_3$)(mPTA)}$_2$-μ-(EBTT-κS7,S′7)](CF$_3$SO$_3$)$_2$ (2)*

Complex **2** was synthesized by the same procedure described above for **1**. The purine derivative $EBTTH_2$ (0.0103 g, 0.023 mM) was reacted with [RuClCp(PPh_3)(mPTA)](CF_3SO_3) (0.0285 g, 0.036 mM) to give a yellow powder.

Yield: 36 mg, 80%. $S_{25,H2O}$ (mg/cm^3): 0.75. Log *P*: 1.1. Elemental analysis for $C_{78}H_{86}F_6N_{14}O_{10}P_4Ru_2S_4$ (1947.89 g M^{-1}): Found C, 47.87; H, 4.36; N, 10.14; S, 6.43%; Calcd C, 48.09; H, 4.45; N, 10.07; S, 6.58%.

IR (KBr, cm^{-1}): *ν*(C6=O) 1683 (s); *ν*(C2=O) 1641 (s); *ν*(C=C+C=N) 1480 (s); *ν*(SC) 1284 (s); *ν*(SO) 1224 (s); ^{1}H NMR (20 °C, DMSO-d$_6$): *δ* 2.74 (bs, C**H**$_3$N$_{mPTA}$, 6H); 2.86–3.10 (m, S–C**H**$_{2(EBTT)}$, 4H); 3.17 (s, N1–C**H**$_{3(EBTT)}$,6H); 3.34 (s, N3–C**H**$_{3(EBTT)}$, 6H);

3.40–4.28 (m, C**H**$_2$P$_{mPTA}$, 12H); 4.82–4.98 (m, C**H**$_2$N$_{mPTA}$, 12H); 5,26 (s, Cp, 10H); 7.23–7.58 (m, aromatics, 30H). ^{13}C{^{1}H} NMR (20 °C, DMSO-d$_6$): δ 27.93 (s, N1–CH$_{3(EBTT)}$); 30.22 (s, N3–CH$_{3(EBTT)}$); 32.21 (s, S–**C**H$_{2(EBTT)}$); 49.03 (s, C**H$_3$**N$_{mPTA}$); 50.68 (d, $^1J_{CP}$ = 15.30 Hz, N**C**H$_2$P$_{mPTA}$); 52.07 (bs, CH$_3$N**C**H$_2$P$_{mPTA}$); 59.80 (s, CH$_3$N**C**H$_2$N$_{mPTA}$); 68.14 (s, N**C**H$_2$N$_{mPTA}$); 85.77 (s, C$_p$); 119.65 (q, $^1J_{CF}$ = 315.82 Hz, OSO$_2$CF$_3$]; 112.65 (s, C5); 129.16–133.81 (m, aromatics); 150.11 (s, C4); 151.67 (s, C8); 152.80 (s, C6); 155.28 (s, C2). ^{31}P{^{1}H} NMR (20 °C, DMSO-d$_6$): δ 42.37 (d, $^2J_{PP}$ = 38.04 Hz); −18.00 (d, $^2J_{PP}$ = 38.04 Hz). Cyclic voltammetry (DMF, 22 °C): $E_{ox(1)}$ = 0.558 mV; $E_{ox(2)}$ = 0.736 mV; E$_{red(2)}$ = 0.697 mV; E$_{1/2(2)}$ = 0.716 mV.

2.4. *Synthesis of [{RuCp(PPh$_3$)(mPTA)}$_2$-μ-(PBTT-κS7,S′7)](CF$_3$SO$_3$)$_2$ (3)*

The purine derivative PBTTH$_2$ (0.019 g, 0.040 mM) was reacted with [RuClCp(PPh$_3$)(mPTA)](CF$_3$SO$_3$) (0.058 g, 0.074 mM) by the same procedure for synthesizing the previous complexes, resulting in a yellow powder.

Yield: 60 mg, 75%. S$_{25,H2O}$(mg/cm^3): 0.7. Log *P*: 1.2. Elemental analysis for C$_{79}$H$_{88}$F$_6$N$_{14}$O$_{10}$P$_4$Ru$_2$S$_4$ (1961.12 g M^{-1}): Found C, 47.85; H 4.41; N 9.83; S 6.51%; Calcd C, 48.36; H, 4. 52; N, 10.00; S, 6.54%.

IR (KBr, cm^{-1}): *ν*(C6=O) 1683 (s); *ν*(C2=O) 1634 (s); *ν*(C=C+C=N) 1521 (s); *ν*(SO) 1228 (s); ^{1}H NMR (20 °C, DMSO-d$_6$): δ 2.08 (q, S–CH$_2$–C**H**$_{2(PBTT)}$, 2H); 2.67 (bs, C**H**$_3$N$_{mPTA}$, 6H); 3.18 (s, N1–C**H**$_{3(PBTT)}$, 6H); 3.32 (s, N3–C**H**$_{3(PBTT)}$, 6H); 3.37 (m, S–C**H**$_{2(PBTT)}$, 4H); 3.71–3.82 (m, C**H**$_2$P$_{mPTA}$, 12H); 4.06–4.20 (m, C**H**$_2$N$_{mPTA}$, 12H); 4.55 (s, Cp, 10H); 7.30–7.52 (m, aromatics, 30H). ^{13}C{^{1}H} NMR (20 °C, DMSO-d$_6$): δ 28.07 (s, N1–CH$_{3(PBTT)}$); 29.73 (s, S–CH$_2$–CH$_{2(PBTT)}$); 30.05 (s, N3–CH$_{3(PBTT)}$); 30.52 (s, S–**C**H$_{2(PBTT)}$); 48.71 (s, CH$_3$N$_{mPTA}$); 51.83 (d, $^1J_{CP}$ = 15.5 Hz, NCH$_2$P$_{mPTA}$); 52.37 (d, $^1J_{CP}$ = 12.5 Hz, CH$_3$N**C**H$_2$P$_{mPTA}$); 59.50 (s, CH$_3$N**C**H$_2$N$_{mPTA}$); 63.40 (s, N**C**H$_2$N$_{mPTA}$); 79.55 (s, Cp); 119.82 (q, $^1J_{CF}$ = 319.95 Hz, OSO$_2$CF$_3$); 108.20 (s, C5); 128.55–133.52 (m, aromatics); 148.60 (s, C4); 148.91 (s, C8); 151.23 (s, C6); 153.64 (s, C2). ^{31}P{^{1}H} NMR (20 °C, DMSO-d$_6$): δ −15.50 (d, $^2J_{PP}$ = 44.00 Hz); 47.43 (d, $^2J_{PP}$ = 44.00 Hz). Cyclic voltammetry (DMF, 22 °C): $E_{ox(1)}$ = 0.420 mV; $E_{ox(2)}$ = 0.730 mV.

2.5. *Stability tests of the complexes with O$_2$ and H$_2$O*

The obtained ruthenium complexes were air stable for months in the solid state and for two days in solution. In a standard procedure, 0.01 g of **1**, **2**, and **3** were introduced into a 5 mm NMR tube and dissolved in 0.5 mL of CDCl$_3$. The resulting solution was cooled to 0 °C and then dry O$_2$ was bubbled throughout the solution for 2 min via a long syringe needle. ^{31}P{^{1}H} NMR showed that no significant changes were produced in two days at room temperature. No decomposition was observed after two days at 40 °C as well. Sequential additions of 50 μL of DMSO-d$_6$ and D$_2$O into the CDCl$_3$ solution did not produce any significant change in the starting complexes after two days at 40 °C.

2.6. *Cyclic voltammetry experiments*

Electrochemical experiments were performed with a VersaSTAT3 apparatus. A standard disposition for the measurement cell was used including a three-electrode glass cell consisting of a platinum disk-working electrode, a platinum-wire auxiliary electrode, and an Ag reference electrode. The supporting electrolyte solution (LiClO$_4$, 0.05 M) was scanned over the

solvent window to verify the absence of electro-active impurities. A similar concentration of the analyte (0.1 mM) in DMF was employed in all the measurements.

2.7. *Octanol–water partition coefficient determination*

The octanol–water partition coefficient of the ruthenium complexes was obtained by a slow-stirring method that provides accurate Log *P* results over a wide range of concentration values [38–40]. The procedure was adapted to the solubility properties of the complexes. Solutions of the complexes between 10^{-4} and 10^{-3} M were prepared in octanol previously saturated with distilled water. Into a 40 mL container with a magnetic stir bar was introduced initially 10 mL of the water phase previously saturated with octanol and then by a syringe 10 mL of the octanol one so that the solution did not emulsify. The container was closed with a silicone septum and stirred slowly at 25 ± 1 °C. Samples were taken from the octanol and water phases with a syringe through the septum periodically until the concentrations in both phases stabilized. Concentrations of the complex in each phase were measured using UV–vis spectroscopy.

2.8. *DNA mobility shift assay*

Reactions between ruthenium complexes and DNA were performed in 20 µL of 10 mM phosphate buffer solution at pH 7.0 containing 1 µg of Bluescript KSII plasmid (3Kbp, from Stratagene), and the appropriate amounts of a freshly prepared water solution of the complex to achieve the desired metal-to-base pair stoichiometry. Reaction mixtures were incubated for 16 h at 37 °C and 10 µL of the samples were analyzed by electrophoresis in 1% agarose-TAE gels. DNA bands were visualized by staining with ethidium bromide and photographed under UV light. For each active compound, the Ri value (metal to base molar ratio at the onset of the incubation), at which complete transformation of the supercoiled to the relaxed form of the plasmid, was registered.

3. Results and discussion

3.1. *Synthesis and characterization of 1–3*

The dinuclear ruthenium complexes [{RuCp(PPh_3)(mPTA)}$_2$-µ-(*L*-κ*S7,S′7*)](CF_3SO_3)$_2$ (*L* = $MBTT^{2-}$ (**1**), $EBTT^{2-}$ (**2**), and $PBTT^{2-}$ (**3**)) were obtained by reaction of bis-thiopurines $MBTTH_2$, $EBTTH_2$, and $PBTTH_2$ with KOH and [RuClCp(PPh_3)(mPTA)](CF_3SO_3) in refluxing ethanol (scheme 2).

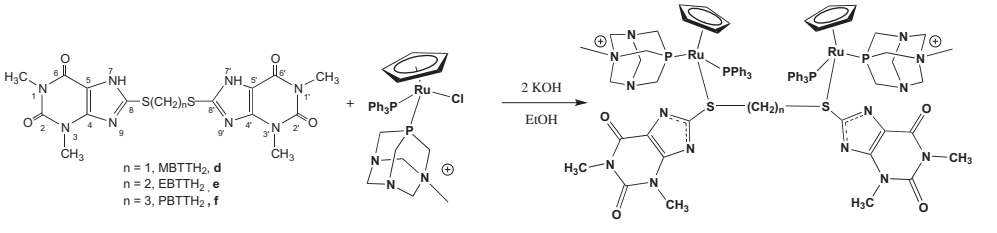

Scheme 2. Synthesis of **1**, **2**, and **3**.

The obtained yellow bimetallic products are air stable in the solid state for months as well as in $CDCl_3$ for more than two days, also containing D_2O and DMSO-d_6 at room temperature and 40 °C. They are soluble in chloroform and DMSO, and slightly soluble in water, methanol, and ethanol. The mPTA ligand provides to the complexes somewhat more solubility in water than PTA in previously published ruthenium complexes such as [{RuCp(PPh_3)(PTA)}$_2$-μ-(*L*-κ*S7,S′7*)] and [{RuCp(PTA)$_2$}$_2$-μ-(*L*-κ*S7,S′7*)] [30].

The elemental analyses of the complexes were in agreement with a proportion of two $\{CpRuLL'\}^+$ (L = PPh_3, PTA; L′ = PTA) units to one bis-thiopurine molecule. The metals coordinate to four different ligands and therefore, they are chiral centers. The obtained products are mixtures of stereoisomers that were not separated. The $^{31}P\{^1H\}$ NMR spectra for the three complexes display two doublets due to the reciprocally coupled mPTA and PPh_3 supporting that both ligands are bonded to the same metal nucleus [**1**: −17.95 ppm, 42.60 ppm (d, $^2J_{PP}$ = 38.52 Hz); **2**: −18.00 ppm, 42.37 ppm (d, $^2J_{PP}$ = 38.04 Hz); **3**: −15.50 ppm, 47.43 ppm (d, $^2J_{PP}$ = 44.00 Hz)]. The ^1H NMR (DMSO-d_6) signals only could be assigned using ^1H, ^1H-2D COSY NMR, and by comparison with those for the parent previously published bimetallic Ru complexes, [{RuCp(PPh_3)(PTA)}$_2$-μ-(*L*-κ*S7,S′7*)] and [{RuCp(PTA)$_2$}$_2$-μ-(*L*-κ*S7,S′7*)]. The ^1H NMR is in agreement with the formation of different stereoisomers, depending on the distribution of the ligands around the metal, producing broader signals than those found in the free ligands. The resonances for N1–CH_3 and N3–CH_3 had similar chemical shifts to those in similar published complexes [30]. The MBTTH$_2$ S–CH_2–S group in **1** was a broad singlet at 4.68 ppm, which is in the range found for [{RuCp(PPh_3)(PTA)}$_2$-μ-(*L*-κ*S7,S′7*)] and [{RuCp(PTA)$_2$}$_2$-μ-(*L*-κ*S7,S′7*)] (4.62 ppm) [30], *cis*-[{PtCl(PPh_3)$_2$}$_2$(μ-MBTT-κ*N7,N7′*)] (5.0 ppm), *cis*-[{Pt(PTA)$_2$}$_2$(μ-Cl)(μ-MBTT-κ*N7,N7′*)]Cl (4.21 ppm) [36], and *trans*-[{PdCl(PPh_3)$_2$}$_2$(μ-MBTT-κ*N7,N7′*)] (4.15 ppm) [32]. In **2**, the four S–$(CH_2)_2$–S protons are chemically different and arise as multiplets from 2.86 to 3.10 ppm, similar to those for ruthenium complexes containing this ligand, Cp, and PTA [30]. In the few known $EBTT^{2-}$ complexes with other metals, a broad singlet was observed for this group: *trans*-[{PdCl(PPh_3)$_2$}$_2$(μ-EBTT-κ*N7,N′7*)] (δ S–$(CH_2)_2$–S: 2.87 ppm) [32] and *cis*-[{Pt(PTA)$_2$}$_2$(μ-Cl)(μ-EBTT-κ*N7,N7′*)]Cl (δ S–$(CH_2)_2$–S: 1.92 ppm) [24]. This fact suggests that $EBTT^-$ coordinates more through the closer sulfur, which are bonded to the –CH_2–CH_2– group, than through the distant N7. In **3**, the S–$(CH_2)_3$–S ^1H NMR signals arose also as multiplets at chemical shifts (δ –CH_2– = 2.08 ppm, δ S–CH_2– = 3.37 ppm) quite different to those for free PBTTH$_2$ (δ –CH_2– = 2.17, S–CH_2– = 3.40 ppm) and coordinated $PBTT^{2-}$ in complexes such as *cis*-[{Pt(PTA)$_2$}$_2$(μ-Cl)(μ-PBTT-κ*N7,N′7*)]Cl (δ –CH_2– = 2.03, S–CH_2– = 3.39 ppm) [24], and *trans*-[{PdCl(PPh_3)$_2$}$_2$(μ-PBTT-κ*N7,N′7*)] (δ –CH_2– = 2.56, S–CH_2– = 3.72 ppm) [32]. Nevertheless, this chemical shift of these signals is similar to those found for ruthenium complexes containing PTA and Cp. This fact suggests newly that sulfurs are the probable coordination point of $PBTT^-$ in **3**.

In contrast, the $^{13}C\{^1H\}$ NMR spectrum of **1** shows the S–CH_2–S and C8 signals (δ S–CH_2–S = 35.53 ppm, C8 = 151.12 ppm) with a chemical shift very close to those found for *cis*-[{Pt(PTA)$_2$}$_2$(μ-Cl)(μ-MBTT-κ*N7,N7′*)]Cl (δ S–CH_2–S = 35.85, C8 = 150.52 ppm) [24] and *trans*-[{PdCl(PPh_3)$_2$}$_2$(μ-MBTT-κ*N7,N7′*)] (δ S–CH_2–S = 36.90, C8 = 150.30 ppm), and published 8MBTT-Cp-PTA ruthenium complexes [30]. While in **2**, the S–$(CH_2)_2$–S and C8 signals (δ S–$(CH_2)_2$–S = 32.21, C8 = 151.67 ppm) are similar to those for free EBTTH$_2$ (δ S–CH_2–S = 32.00, C8 = 148.10 ppm) and the reported complexes *cis*-[{Pt(PTA)$_2$}$_2$(μ-Cl)(μ-N,N-EBTT)]Cl (δ S–$(CH_2)_2$–S = 35.85, C8 = 150.52 ppm) [24] and *trans*-[{PdCl(PPh_3)$_2$}$_2$(μ-EBTT-κ*N7,N′7*)] (δ S–$(CH_2)_2$–S = 32.70, C8 = 150.90 ppm) [32]. Complex **3**

displays a similar $^{13}C\{^{1}H\}$ NMR spectrum to those previously published for similar complexes but for the mPTA-CH_3 signal and some groups that probably are affected by the charge on mPTA. For example, the chemical shifts of the bridging –CH_2– and C8 carbons in **3** (δ –CH_2– = 29.73 ppm; C8 = 148.91 ppm) are similar to those for $[\{RuCp(PTA)_2\}_2$-μ-(PBTT-κ*S7,S′7*)$]^{2+}$ (δ –CH_2– = 28.30 ppm; C8 = 149.73 ppm) but those signals for S–CH_2– in both complexes display quite different chemical shifts (respectively: 30.52 and 45.87 ppm) [30]. Nevertheless, the three discussed groups have a comparable chemical shift to those in **3**, $PBTTH_2$ (δ –CH_2– = 29.20 ppm; S–CH_2– = 30.20 ppm; C8 = 148.20 ppm) and in the reported complexes *cis*-$[\{Pt(PTA)_2\}_2$(μ-Cl)(μ-PBTT-κ*N7,N′7*)]Cl (δ –CH_2– = 32.00 ppm; S–CH_2– = 32.20 ppm; C8 = 151.86 ppm) [24] and *trans*-$[\{PdCl(PPh_3)_2\}_2$(μ-PBTT-κ*N7,N′7*)] (δ –CH_2– = 28.60 ppm; S–CH_2– = 30.40 ppm; C8 = 151.00 ppm) [32].

Due to the poor quality of the crystals resulting from many recrystallization attempts, the single X-ray crystal structures for these complexes were not possible to be obtained. However, the spectroscopic evidence supports that the most probable structures for **1–3** are those displayed in scheme 2, where each S of the bis-8-thio-theophylline derivative is bonded to a Ru, which completes its coordination geometry with an η^5-Cp, a PPh_3, and a mPTA.

3.2. *Electrochemistry of 1–3*

The redox behavior of **1–3** in DMF was studied to find additional evidence for their proposed structures, to obtain information on the redox behavior of two ruthenium metals bonded to close purines in comparison with the parent mono-ruthenium-thio-purine complexes, and to know if their redox properties are similar to those for parent Ru complexes active against DNA.

Complexes **1** and **3** exhibited an irreversible behavior but **2** showed an interesting reversible wave (figure 1). All the recorded electrode potentials were in a short range for the three complexes and similar to those found for mono-ruthenium complexes containing Cp and PTA [41].

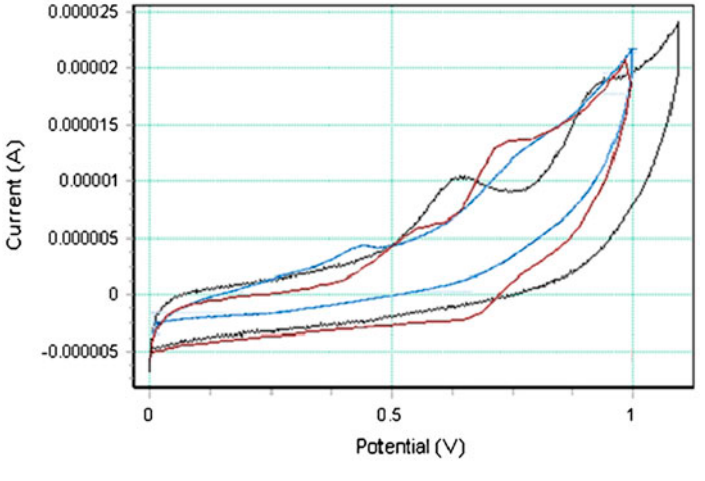

Figure 1. Cyclic voltammograms in DMF of **1** (black line), **2** (red line), and **3** (blue line) (see http://dx.doi.org/10.1080/00958972.2014.947970 for color version).

The two oxidation waves for the complexes only can be assigned to single-electron charge transfer of two independent Ru centers ($Ru^{II}Ru^{II}$ $Ru^{III}Ru^{II}$ $Ru^{III}Ru^{III}$) and therefore, support the proposed bimetallic character for the complexes. The only observed reduction wave, for **2**, is without doubt consequence of the reduction process $Ru^{III}Ru^{III} \rightarrow Ru^{III}Ru^{II}$ that in combination with the oxidation partner represents a reversible redox process [42, 43].

It is interesting to stress that the oxidation potentials decrease linearly when the bispurine-alkyl-bridging group increases in length [$E_{ox(1)}$ = 635 mV (**1**), 558 mV (**2**), 420 mV (**3**); $E_{ox(2)}$ = 920 mV (**1**), 736 mV (**2**), 730 mV (**3**)]. The alkyl size and, therefore, the link size between purines have a clear influence on the redox properties of the $\{CpRu(PPh_3)(mPTA)\}^+$ moiety (figure 2). There are no electronic connections between both metals through the alkyl bridging group and the solvent. Therefore, the observed correlation between the observed redox potentials and the alkyl linking group size could be attributed to steric effects that lead to different conformations for each complex.

3.3. *Reactivity of 1, 2, and 3 with DNA*

The redox properties of the complexes are in the range observed for active anticancer ruthenium complexes [42]. Nevertheless, it is known that the reductive environment found in tumors will favor lower oxidation states and then, Ru^{II} compounds may have less susceptibility for metabolic degradation and longer survival time, until they reach the cancer cells. Therefore, it is expected that in a family of antitumoral ruthenium(II) compounds, a higher oxidation potential should, in principle, correlate with an increase in DNA activity. Previous studies on Pt and Ru complexes [25] have shown that the modification of the electrophoretic mobility of plasmid DNA on agarose gels is commonly taken as confirmatory evidence for a direct DNA–metal interaction. The alteration of the DNA structure leads to unwinding of the plasmid molecule holding up the migration of supercoiled DNA (SC DNA) and slightly increasing the mobility of the open circular DNA (OC DNA), to a point (coalescence point, CP) where both forms co-migrate. We have investigated the interaction of the new water-soluble ruthenium complexes with SC DNA using the shift mobility assay.

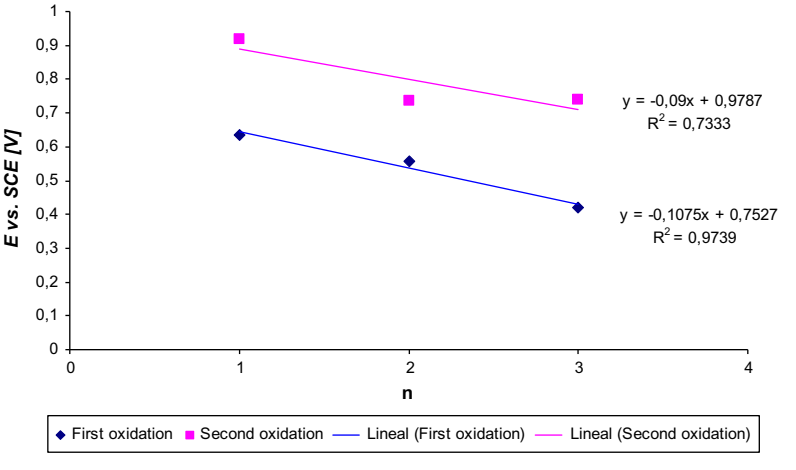

Figure 2. First and second oxidation potential *vs*. the numbers of alkyl group atoms for **1**, **2**, and **3**.

Reactions between the ruthenium complexes and SC plasmid DNA were performed in water buffered with phosphate at pH 7.0 for 14 h at 37 °C and then samples were analyzed by electrophoresis in agarose-TAE gels. The reaction was performed in the dark, although no photochemical activation of the present ruthenium complexes has been observed in contrast to other ruthenium complexes [25].

A delay of SC DNA was observed for **1**, **2**, and **3**. In addition, a modest increase in the amount of the OC DNA is observed, relative to the untreated DNA, indicating that some DNA cleavage may also occur. As mentioned above, ruthenium complexes **1**, **2**, and **3** are stable in water for more than two days at 40 °C in diffuse daylight. Therefore, the complexes are stable and the lack of anticancer activity could not be a consequence of complex decomposition. Tests with the *cis*platin-sensitive cells T2 show that mono-ruthenium complexes containing one PTA and one PPh_3 display significantly better activity than those containing two PTA. This fact was also observed for PTA–Pt complexes and it is probably related to the difficulty for hydrophilic PTA complexes to interact with DNA and in living cell for crossing the lipophilic membranes of the cell and cell nucleus to reach their target, the nucleic acids. The found anticancer activity of the parent complexes [{RuCp(PPh_3)(PTA)}$_2$-μ-(*L*-κ*S7,S′7*)] and [{RuCp(PTA)$_2$}$_2$-μ-(*L*-κ*S7,S′7*)] [30] were not significant, which is in agreement with their Log *P*. A different combination of phosphines bonded to the metal could lead to a more convenient distribution between water and organic solvents. The Log *P* found for **1**, **2**, and **3** were similar and *c.a.* 1 (Log *P*: 0.94 (**1**); 1.1 (**2**); 1.2 (**3**)) indicating that these complexes are not significantly distributed between organic and water phases. The found data support the hypothesis that the liphophilic/hydrophilic balance could be a determining factor for the biological activity trend inside the group of the Ru complexes examined in this paper.

4. Conclusion

The present work details the synthesis of the first examples of binuclear Cp-ruthenium(II) complexes bearing the bis-thiopurines, bis-thiopurines-bis(S-8-thiotheophyllinate)methane ($MBTT^{2-}$), 1,2-bis(S-8-thiotheophyllinate)ethane ($EBTT^{2-}$), and 1,3-bis(S-8-thiotheophyllinate)propanealkane ($EPTT^{2-}$), and the ligands mPTA and PPh_3. These complexes display more water solubility than those similar ruthenium complexes containing PTA. The three complexes show two successive one-electron oxidations ($Ru^{II}Ru^{II}/Ru^{III}Ru^{II}$ and $Ru^{III}Ru^{II}/Ru^{III}Ru^{III}$), in agreement with the presence of two metals in the molecule. The redox potentials of the complexes decrease linearly increasing the bridging alkyl size of the bis(8-thiotheophylline) ligands, which is most probably justified by steric effects. The complexes display very low activity against DNA that could be justified by their partition coefficients (Log *P*) that indicate that the lipophilic/lipophobic balance for the complexes are not adequate for reaction with DNA. On this basis, it is imaginable that an adequate combination of phosphines could afford DNA-active water-soluble Cp-ruthenium complexes containing bisthiopurines. Studies in this direction are in progress in our laboratory.

Acknowledgements

Financial support co-financed by the EU FEDER: Thanks are given to the Spanish MINECO (project CTQ2010-20952) and Junta de Andalucía (PAI research teams FQM-317 and

Excellence Projects P07-FQM-03092 and P09-FQM-5402). Thanks are also given to COST Action CM1302 (WG1, WG2). M. Serrrano-Ruiz is grateful to Junta de Andalucía for the postdoctoral contract in the frame of the project P09-FQM-5402.

References

[1] B. Rosenberg, L. Van Camp, T. Krigas. *Nature*, **205**, 698 (1965).
[2] B.S. Howerton, D.K. Heidary, E.C. Glazer. *J. Am. Chem. Soc.*, **134**, 8324 (2012).
[3] K.J. Kilpin, C.M. Clavel, F. Edafe, P.J. Dyson. *Organometallics*, **31**, 7031 (2012).
[4] M. Carreira, R. Calvo-Sanjuán, M. Sanaú, I. Marzo, M. Contel. *Organometallics*, **31**, 5772 (2012).
[5] T. Mihály, M. Garijo-Añorbe, F.M. Albertí, P.J. Sanz-Miguel, B. Lippert. *Inorg. Chem*., **51**, 10437 (2012).
[6] H.-C. Tai, R. Brodbeck, J. Kasparkova, N.J. Farrer, V. Brabec, P.J. Sadler, R.J. Deeth. *Inorg. Chem.*, **51**, 6830 (2012).
[7] R. Gaur, L. Mishra. *Inorg. Chem.*, **51**, 3059 (2012).
[8] J. Vícha, G. Demo, R. Marek. *Inorg. Chem.*, **51**, 1371 (2012).
[9] K. Kam-Wing Lo, A. Wing-Tat Choi, W. Ho-Tin Law. *Dalton Trans*., 6021 (2012).
[10] N.J. Farrer, L. Salassa, P.J. Sadler. *Dalton Trans.*, 10690 (2009).
[11] E.R. Jamieson, S.J. Lippard. *Chem. Rev.*, **99**, 2467 (1999).
[12] B. Stordal, M. Davey. *IUBMB Life*, **59**, 696 (2007).
[13] N. Pabla, Z. Dong. *Kidney Int.*, **73**, 994 (2008).
[14] S. Betanzos-Lara, L. Salassa, A. Habtemariam, P.J. Sadler. *Chem. Commun.*, **45**, 6622 (2009).
[15] G.I. Pascu, A.C.G. Hotze, C. Sanchez-Cano, B.M. Kariuki, M.J. Hannon. *Angew. Chem. Int. Ed.*, **46**, 4374 (2007).
[16] W.H. Ang, P.J. Dyson. *Eur. J. Inorg. Chem.*, **2006**, 4003 (2006).
[17] Y.K. Yan, M. Melchart, A. Habtemariam, P.J. Sadler. *Chem. Commun.*, **42**, 4764 (2005).
[18] A.C.G. Hotze, S.E. Caspers, D. de Vos, H. Kooijman, A.L. Spek, A. Flamigni, M. Bacac, G. Sava, J.G. Haasnoot, J. Reedijk. *J. Biol. Inorg. Chem.*, **9**, 354 (2004).
[19] R.E. Morris, P.J. Sadler, H. Chen, D. Jodrell, *US Patent*, 6750 251 B2 (2004).
[20] E. Alessio, G. Mestroni, A. Bergamo, G. Sava. *Curr. Top. Med. Chem.*, **4**, 1525 (2004).
[21] E. Alessio, G. Mestroni, A. Bergamo, G. Sava. *Met. Ions Biol. Syst.*, **42**, 323 (2004).
[22] C.G. Hartinger, S. Zorbas-Seifried, M.A. Jakupec, B. Kynast, H. Zorbas, B.K.J. Keppler. *Inorg. Biochem.*, **100**, 891 (2006).
[23] A. Romerosa, P. Bergamini, V. Bertolasi, A. Canella, M. Cattabriga, R. Gavioli, S. Mañas, N. Mantovani, L. Pellacani. *Inorg. Chem.*, **43**, 905 (2004).
[24] P. Bergamini, V. Bertolasi, L. Marvellli, A. Canella, R. Gavioli, N. Mantovani, S. Mañas, A. Romerosa. *Inorg. Chem.*, **46**, 4267 (2007).
[25] A. Romerosa, T. Campos-Malpartida, C. Lidrissi, M. Saoud, M. Serrano-Ruiz, M. Peruzzini, J.A. Garrido-Cardenas, F. Garcia-Maroto. *Inorg. Chem.*, **45**, 1289 (2006).
[26] A. Mena-Cruz, P. Lorenzo-Luis, A. Romerosa, M. Saoud, M. Serrano-Ruiz. *Inorg. Chem.*, **46**, 6120 (2007).
[27] A. Mena-Cruz, P. Lorenzo-Luis, A. Romerosa, M. Serrano-Ruiz. *Inorg. Chem.*, **47**, 2246 (2008).
[28] A. Mena-Cruz, P. Lorenzo-Luis, V. Passarelli, A. Romerosa, M. Serrano-Ruiz. *Dalton Trans.*, 3237 (2011).
[29] M. Serrano-Ruiz, L.M. Aguilera-Sáez, P. Lorenzo-Luis, J.N. Padrón, A. Romerosa. *Dalton Trans.*, 11212 (2013).
[30] L. Hajji, C. Saraiba-Bello, A. Romerosa, G. Segovia-Torrente, M. Serrano-Ruiz, P. Bergamini, A. Canella. *Inorg. Chem.*, **50**, 873 (2011).
[31] D.D. Perrin, W.L.F. Armarego (Eds.). *Purification of Laboratory Chemicals*, 3rd Edn, Butterworths and Heinemann, Oxford (1988).
[32] A. Romerosa, C. López-Magaña, A.E. Goeta, S. Mañas, M. Saoud, F.B. Benbdelouahab, F. El Guemmout. *Inorg. Chim. Acta*, **353**, 99 (2003).
[33] B. Cornils, W.A. Herrmann (Eds.). *Aqueous-Phase Organometallic Catalysis*, Wiley-VCH, Weinheim (1998).
[34] F. Joo, J. Kovacs, A. Katho, A.C. Benyei, T. Decuir, D.J. Darensboug. *Inorg. Synth.*, **32**, 2 (1998).
[35] A. Romerosa, C. López-Magaña, M. Saoud, E. Colacio, J. Suarez-Varela. *Inorg. Chim. Acta*, **307**, 125 (2000).
[36] A. Romerosa, C. López-Magaña, M. Saoud, S. Mañas. *Eur. J. Inorg. Chem.*, **2003**, 348 (2003).
[37] A. Romerosa, C. López-Magaña, S. Mañas, M. Saoud, A.E. Goeta. *Inorg. Chim. Acta*, **353**, 145 (2003).
[38] R. Mannhold, G.I. Poda, C. Ostermann, I.G. Tetko. *J. Pharm. Sci.*, **98**, 861 (2009).
[39] H.R. Lozano, F. Martínez, F. Braz. *J. Pharm. Sci.*, **42**, 601 (2006).
[40] L. Ropel, L.S. Belveze, S.N.V.K. Aki, M.A. Stadtherr, J.F. Brennecke. *Green Chem.*, **7**, 83 (2005).
[41] V. Gutkin, J. Gun, P.V. Prikhodchenko, O. Lev, L. Gonsalvi, M. Peruzzini, A. Romerosa, T. Malpartida, C. Lidrissi. *J. Electrochem. Soc.*, **154**, F7 (2007).
[42] M. Auzias, B. Therrien, G. Süss-Fink, P. Štěpnička, W.H. Ang, P.J. Dyson. *Inorg. Chem.*, **47**, 578 (2008).
[43] M. Gras, B. Therrien, G. Süss-Fink, P. Štěpnička, A.K. Renfrew, P.J. Dyson. *J. Organomet. Chem.*, **693**, 3419 (2008).